

Single- and multiple-electron-loss-cross-section measurements from 20-MeV Fe^{4+} on thin gaseous targets

G. D. Alton, L. B. Bridwell,* M. Lucas,[†] C. D. Moak, P. D. Miller, C. M. Jones, Q. C. Kessel,[‡] A. A. Antar,[‡] and M. D. Brown[§]

Oak Ridge National Laboratory, Oak Ridge, Tennessee 37830

(Received 28 July 1980)

Single- and multiple-electron-loss cross sections have been measured with 20-MeV Fe^{4+} on thin He, Ne, Ar, Kr, Xe, H₂, N₂, O₂, CH₄, CO₂, CHF₃, CF₄, and SF₆ gaseous targets; cross-section-per-atom data for each system are presented. Cross-section-per-atom data from targets with approximately the same average atomic number indicate that both "nonadditivity" and "density" effects, depending on the final charge state of the ion, play roles in electron-loss processes during projectile interactions with molecular targets. A modified Bohr formula is developed which reproduces single-electron-loss-per-atom data for atomic targets.

I. INTRODUCTION

The study of processes which occur during interactions of high-energy particles with matter such as scattering, energy transfer, and associated radiation and ionization phenomena, has provided much of the fundamental information which has led to our understanding of atomic and molecular structures. Theoretical and experimental analyses of such collisional phenomena have continually progressed since the pioneering work of Thompson and Rutherford. Since that time, considerable efforts have been put forth by many investigators toward improving the understanding of the basic mechanisms which lead to energy loss by heavy particle beams as they penetrate matter. Projectile energy loss, at energies below nuclear excitation levels, is known to be by means of elastic nuclear and electronic encounters, discrete electronic excitation with subsequent radiation, and electron-capture-and-loss processes. Although the relative importance of a particular mechanism depends on the velocity of the particle in the medium under consideration, capture and loss processes are known to be important energy transfer mechanisms at projectile velocities exceeding or of the order of the electron orbital velocities associated with the projectile. These processes, therefore, play an important part in projectile deceleration at these energies and corresponding cross-section information is of particular relevance to the study of projectile stopping power and channeling phenomena—areas which have received considerable attention over the years.

Charge changing in the projectile velocity region $v_0 \leq v \leq z_1 v_0$ is of considerable practical importance to the accelerator engineer and user who benefits by the disparity between multiple-electron-loss-and-capture processes as a means of increasing the beam intensity in a given charge state and thus the energy of the ion beam in these devices (z_1 is

the atomic number of the projectile, v_0 is the velocity of the first Bohr electron). For such practical applications, it is desirable to allow the beam of particles to pass through a minimum thickness of the particular target so that charge-state equilibrium is established without serious multiple scattering or appreciable modification to the projectile energy.

The subject of equilibrium charge states of heavy ions in solid and gaseous targets has been reviewed by Moak.^{1,2} Comprehensive review articles which contain valuable information on experimental and theoretical equilibrium and nonequilibrium charge-changing processes have been published by Nikolaev,³ primarily for ions with atomic numbers z_1 , $2 \leq z_1 \leq 18$ and by Betz⁴ for heavier systems. Since the last review article, additional information has been published by other investigators.⁵⁻⁸ Rather extensive amounts of data have been accumulated to date on the subject of equilibrium and nonequilibrium charge-state distributions such as those of Datz *et al.*⁹ for many heavy projectiles and projectile energies interacting with gaseous and solid targets. From these data along with the semiempirical formulations of Nikolaev and Dmitriev¹⁰ and more recently Sayer,¹¹ most of the present day accelerator related charge-state information is readily available or can be computed for a variety of projectile, projectile energy, and target combinations.

The complexity of interactions between high velocity multi-electron projectiles and targets has precluded accurate theoretical descriptions of electron-capture-and-loss processes even though attempts have been made by several investigators.¹²⁻¹⁸ Although these efforts have succeeded in describing, at least qualitatively, charge-changing phenomena for high energy, heavy projectile-target combinations, they do not predict cross-section values for these processes quantitatively. The difficulty of such calculations can readily be appreciated when

one considers the very large number of electronic excitation configurations which are energetically possible in these interactions.

The physics of high-energy ion-atom interactions can best be understood when collisional systems are studied under single event conditions and where differential and total scattering cross-section information can be obtained without ambiguity. These criteria dictate the use of dilute gaseous targets because of the very high densities associated with solid targets in which single event conditions cannot be easily met. In order to obtain a complete set of total electron-capture-and-loss cross-section data, several parametric studies must be made including their dependence on projectile atomic number z_1 , projectile energy E (or velocity v), projectile incident charge state q_1 , and average atomic number Z_2 of the target (the latter definition allows for molecular targets). If one wishes to study the dynamics of such interactions, the correlation between charge state and scattering angle must be made. (The studies of Alton *et al.*,⁵ Spicuzza and Kessel,⁸ and Scott *et al.*¹⁹ are illustrative examples.) Although there have been a number of experimental investigations on the subject of electron-capture-and-loss cross sections such as those of Datz *et al.*,⁹ Knudsen *et al.*,⁷ and other investigations cited in Refs. 3 and 4, the amount of data available is very limited compared to the extensive matrix of possible projectile, projectile energy, and target combinations.

The velocity dependences of electron-capture-and-loss cross sections by 0.26–2.8 MeV/amu F^{m+} passing through Ne have been measured by Macdonald *et al.*²⁰ and for 0.42–2.8 MeV/amu F^{m+} interacting with Ar by Ferguson *et al.*²¹ In these studies, the velocity dependence of single- and multiple-electron-capture-and-loss cross sections were determined. Similar measurements have been reported by Tonuma *et al.*²² for N^{4+} and C^{4+} ions of energies between 3.5 and 7.5 MeV/amu. Single-electron-loss cross sections were found to be in reasonable agreement with a modified Bohr formula. Differential and total charge-changing cross sections for 20-MeV F^{5+} and Cl^{4+} on N_2 , Ar, and Xe targets have been reported by Scott *et al.*¹⁹ In this study charge-fraction data were analyzed in terms of their impact-parameter dependences using Bohr, Thomas Fermi, and Lenz-Jensen interaction potentials and the resulting multiple-electron-loss total cross sections compared with those obtained by direct integration of the experimental angular differential cross sections.

Of particular relevance to the present investigations are the thin target measurements of Knudsen *et al.*,⁷ in which multiple-electron-loss cross

sections were obtained from single event interactions between 20-MeV Fe^{4+} and N_2 , Ar, Kr, Xe, and SF_6 targets. Comparisons of the single-loss cross-sections per atom with the Bohr formula predictions were found to agree reasonably well in shape and magnitude. From these measurements, shell effects are readily evident from the changes in shape of the cross-section per atom at closed-shell configurations. For example, there are two regions for which the cross sections for all targets have the same general shape: the regions $4 \leq q \leq 8$ and $9 \leq q \leq 16$ corresponding to charge states below and above the $1s^2 2s^2 2p^6 3s^2 3p^6$ or argonlike ionic configuration. The opening of the neonlike and heliumlike shells are also expected to produce changes in electron-loss cross-section shape in these regions as well.

In the present study, we have chosen to investigate the dependence of total single and multiple-electron-loss cross sections on average atomic number Z_2 —an area that has not been investigated in any systematic manner until recently. In the present study, we have extended the work of Knudsen *et al.*⁷ to lower average atomic number targets and we have examined the influence of molecular targets on electron-loss cross sections. Cross-section data resulting from the interactions of 20-MeV Fe^{4+} with He, Ne, Ar, Kr, Xe, H_2 , N_2 , O_2 , CH_4 , CO_2 , CHF_3 , CF_4 , and SF_6 targets were obtained during these investigations.

II. EXPERIMENTAL APPARATUS, PROCEDURES, AND DATA ANALYSIS

A detailed description of the experimental arrangement identical to the one used in the present study has been given previously by Moak *et al.*⁶ and Knudsen *et al.*,⁷ and therefore only the salient features will be repeated here. The projectile and energy of interest, namely, 20-MeV Fe^{4+} , was produced in the ORNL EN tandem electrostatic accelerator, momentum analyzed, and collimated to a diameter of 1/2 mm immediately before entering a 9.4-cm long differentially-pumped gas cell. After emerging from the cell, individual charge states, from the multiplicity of states produced during projectile passage through the target, were focused by means of a magnetic quadrupole doublet lens through an electrostatic charge-state analyzer and onto a 5 cm-long position-sensitive detector. All components in the system were precisely aligned and tested with the ion beam in order to ensure that no losses occurred during beam transit to the detection system due to quadrupole steering or component misalignment. Prior to data accumulation, quadrupole settings were carefully determined

for each charge state in order to assure the simultaneous detection of all particles of the particular focused charge state while maintaining good spatial resolution between adjacent charge states. In practice, charge states +3 and +10 could be easily resolved simultaneously and totally collected whenever the quadrupole setting was made for the +10 component. The procedure permitted fast accumulation of data and eliminated the necessity of incorporating a beam monitor system required in previous experiments. Due to the fact that all charge states could be simultaneously collected on the detector, the charge-state yields were measured on an absolute basis. The limiting acceptance angle subtended from the center of the gas cell to the entrance to the quadrupole was 8 mrad, sufficient for transmission of all scattered particles leaving the cell. Cell pressures were measured with a standard capacitance manometer and feedback control system with typical observed variations in the set pressure of $\leq 2\%$. Pressures were recorded at the beginning and end of each measurement and the average value taken as the cell pressure during the measurement. Beam-line pressures preceding and following the gas cell were typically $\sim 2 \times 10^{-6}$ Torr reducing the $q=4$ charge-state component with no gas in the cell to $\sim 97\%$. The effects produced by the residual beam-line pressures and resulting primary charge-state contamination were accounted for in the data analysis.⁷

Charge-state yield measurements were made over a pressure range of 0–10 m Torr for each of the gases investigated in order to determine the linear region of yield with pressure for each charge state and thus, to assure the measurement of single event processes. Data which deviated from the linearity criterion were not used in cross-section determinations. In order to take into account the effect produced by the residual gas and resulting "zero"-pressure charge-state contamination of the initial $q=4$ beam, the initial growth method described by Knudsen *et al.*⁷ was used in analyzing the data. Corrections were made by assuming that the residual beam-line pressure P_0 produced the same yield of a given charge state as an equivalent amount of the target gas of interest. Since P_0 is derived anew for each value of q , it is the pressure of target gas which is equivalent to the residual gas for that charge state, and the results do not depend on the nature of the background gas. Systematic variations in the yield data were taken into account by comparing results with those of previous runs, including repetition of some of the Knudsen *et al.* data and found to be in agreement within $\pm 10\%$.

The total cross section $\sigma_{4 \rightarrow \text{total}}$ for attenuation of the incident $q=4$ charge state is a composite sum

of the individual cross sections for all processes and is given by

$$\sigma_{4 \rightarrow \text{total}} = \sum_q \sigma_{4 \rightarrow q} \quad (1)$$

The total loss cross section was determined from the slope of a semilogarithmic plot of the yield of charge state $q=4$ with pressure. A sum of the individual measured cross sections through $q=10$ was found to be less than the measured total by 1–11% in all cases, as they should be, due to the omission of some of the low-probability charge-state cross sections.

III. RESULTS

Single- and multiple-electron-loss cross-section dependences on the atomic number of noble gas targets He, Ne, Ar, Kr, and Xe are shown in Fig. 1. Two distinct regions are evident for each of the final charge states. We note that the cross sections increase almost linearly in the region $2 \leq Z_2 \leq 18$ and again almost linearly between $18 \leq Z_2 \leq 54$. The slight decrease in the cross sections for Kr which are evident are not fully understood. Similar decreases in single-loss cross sections relative to those obtained from Ar targets have been reported by Nikolaev.³

The shell effects associated with electron removal prior and following the $1s^2 2s^2 2p^6 3s^2 3p^6$ or argonlike configuration are illustrated in Fig. 2. Here again, we observe unexpectedly low cross sections for Kr targets relative to those obtained from Ar and Xe for a given charge state.

Electron-loss cross-section-per-atom data versus final projectile charge state are shown in Fig. 3 for neon and the molecular targets, CO_2 , CF_4 , and SF_6 . We note that per atom, the molecular targets are not as effective as neon for producing charge states less than $q=8$ while they are more effective for producing charge states greater

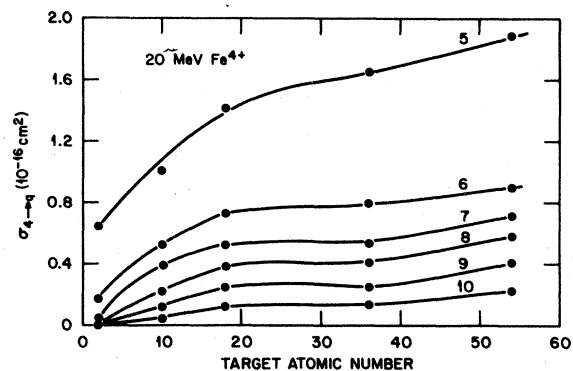


FIG. 1. Single- and multiple-electron-loss cross-section data versus atomic number for He, Ne, Ar, Kr, and Xe target gases.

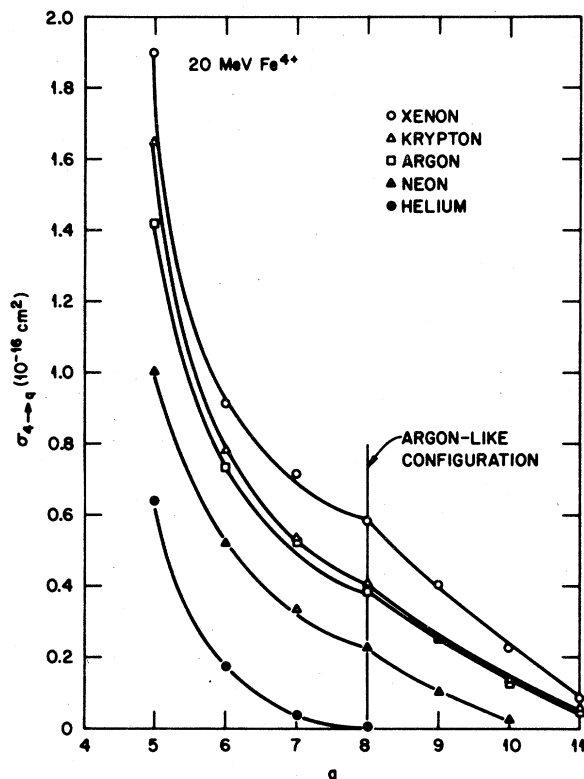


FIG. 2. Electron-loss cross section versus final projectile charge state produced in He, Ne, Ar, Kr, and Xe targets. The data have been plotted on a linear scale in order to illustrate the change in shape of the cross section versus projectile final-charge-state curves at $q=8$. The changes are attributable to the increase in binding energies between the $3d$ and $3p$ subshells and illustrate a so-called "shell effect".

than $q=8$ and are approximately equivalent at $q=8$. The cross-section-per-atom data thus reflects a "nonadditivity" effect for charge states less than $q=8$ and a "density" effect for charge states greater than $q=8$. The latter effect is believed to be due to multiple interactions between the projectile and target constituents.

The remaining multiple-electron-loss-cross-section data acquired during these investigations for other molecular targets relative to those of He, Ne, Ar, Kr, and Xe are shown in Fig. 4. An interesting result is the apparent equivalence of the cross section per atom for H_2 and CH_4 at $q=5$ indicating perhaps that for single loss, the ion essentially interacts with the hydrogen in the CH_4 molecule while the influence of the carbon atom is evident for multiple-electron-loss processes.

IV. SINGLE-ELECTRON-LOSS FORMULA

In his 1948 treatment on the subject of particle penetration in matter, Bohr¹⁷ deduced a formula

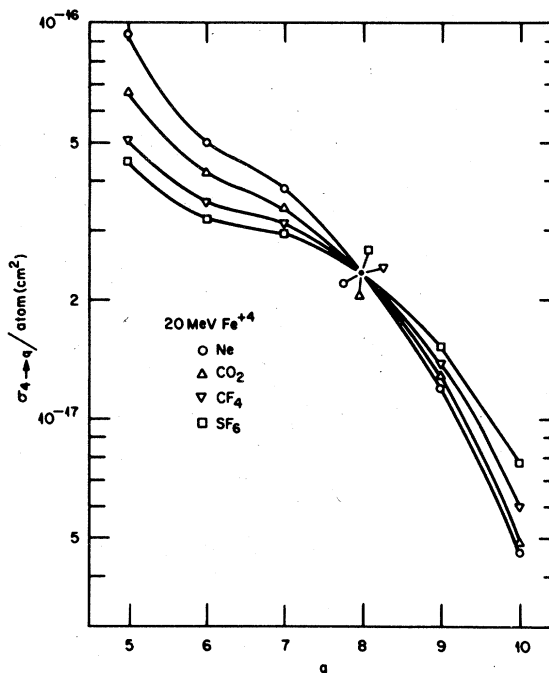


FIG. 3. Comparison of the electron-loss cross-sections-per-atom data produced in CO_2 , CF_4 , and SF_6 with those produced in Ne as a function of final projectile charge state. The data illustrate the "nonadditivity effect" observed in molecular gases for charge states $q < 8$ and a "density effect" for charge states of $q > 8$.

for estimating single-electron-capture-and-loss cross sections which is assumed appropriate for fast heavy ion-heavy atom interpenetrating collisions. Knudsen *et al.*⁷ have shown by comparison with experimental data that the Bohr formula given by

$$\sigma_{\text{Bohr}} (\text{cm}^2) = \pi a_0^2 (Z_1^{1/3} + Z_2^{1/3})^2 (v_0/v_i)^2 \quad (2)$$

agrees reasonably well in shape, but over predicts significantly, single-electron-loss cross sections for 20-MeV Fe^{+4} on N_2 , Ar, Kr, Xe, and SF_6 targets. [In Eq. (2) a_0 is the radius of the first Bohr electron orbital, v_0 is the velocity of the electron in the first Bohr orbital, Z_1 , Z_2 are the atomic numbers of the projectile and target, respectively, and v_i is the velocity of the projectile.] The Bohr formula was intended at best to be a rough estimator of the cross sections for single electron capture or loss during collisions between fast heavy target materials, and it is not at all surprising that cross sectional values do not agree with those experimentally observed. On the other hand, the agreement in shape as found by Knudsen *et al.* predicted by the formula is quite encouraging. The formula, as noted, does not include the effects of electronic binding energies on loss processes and therefore, Eq. (2) should be more appropriate for

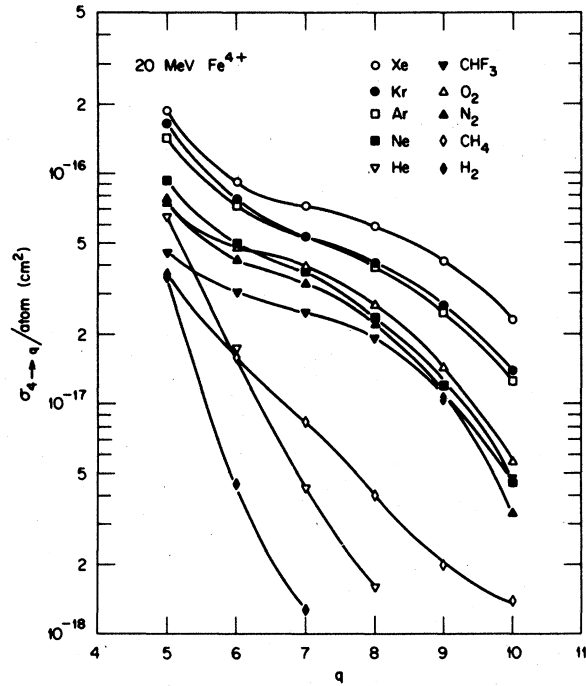


FIG. 4. Electron-loss cross-section-per-atom data versus final projectile charge state produced in He, Ne, Ar, Kr, and Xe atomic and H_2 , CH_4 , N_2 , O_2 , and CHF_3 molecular targets.

more weakly bound electrons than those considered by Knudsen *et al.*⁷

Plausible arguments can be made that cross sections for single-electron loss should be directly proportional to the number of electrons residing in a given subshell N_j , where the individual electronic binding energies are approximately equal. In this case, all electrons have equal probabilities for removal. Furthermore, one can argue that the probability of removal of a particular electron should be inversely proportional to the energy required for removal—i.e., the binding or ionization energy I_j of the electron. Using these arguments and the Bohr formula [Eq. (2)], we can deduce a modified single-electron-loss cross-section formula which should be more appropriate for more tightly bound electrons. The modified formula is given by

$$\sigma_{q \rightarrow q+1} (\text{cm}^2) = N_j \left(\frac{13.6 (\text{eV})}{I_j (\text{eV})} \right) \left(\frac{v_0}{v_j} \right)^2 \times (Z_1^{1/3} + Z_2^{1/3})^2 \pi a_0^2, \quad (3)$$

where the quantity 13.6 is the ionizational potential of the hydrogen atom.

The validities of the previously given arguments were tested by comparing the computed results obtained from Eq. (3) with our measured single-

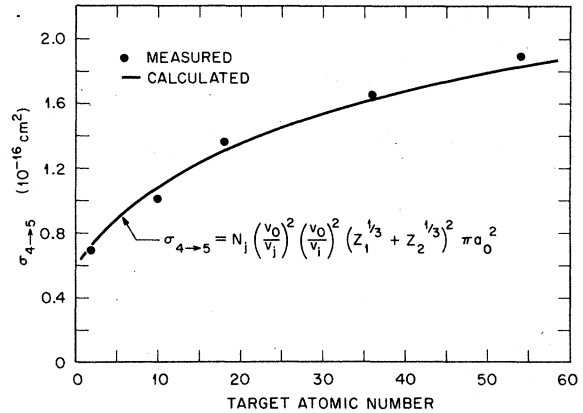


FIG. 5. Comparison of single-electron-loss cross sections computed from the modified Bohr formula [Eq. (3)] with those experimentally measured for He, Ne, Ar, Kr, and Xe targets. (N_j is the number of electrons in the outer subshell which have velocity v_j .)

electron-loss cross-section data. The computed and experimental cross sections for single-electron loss agree surprisingly well both in magnitude and shape as illustrated in Fig. 5. However, further experimental measurements need to be made with other projectile charge states in order to validate these arguments.

V. DISCUSSION AND CONCLUSIONS

The simple Z_2 dependence in Fig. 1 of the cross-section data for the noble gases illustrated would suggest an almost linear dependence for $2 \leq Z_2 \leq 18$ followed by a linear dependence of different slope for $18 \leq Z_2 \leq 54$. These cross sections, which monotonically increase with atomic number, differ from those reported by Nikolaev³ where peaks were observed in the single-electron-loss cross-section data at $Z_2 = 18$ (Ar) for 0.351 and 1.02-MeV He^+ and 1.64-MeV $Ne^{1+ \rightarrow 5+}$ on He, N_2 , Ar, and Kr targets.

From the electron-loss cross-section-per-atom data shown in Fig. 3, it is evident that the effective atomic number of molecular targets as seen by the projectile may be less than or greater than the average atomic number of the molecular system depending on the collisional impact parameter. This is a demonstration of the so-called "non-additivity" effect for projectile electron losses $q \leq 8$ and the "density" effect for $q > 8$ as a result of interactions with more than one atom of the system on the average. At large impact parameters and low final-charge states, the target behaves as if it had an effective Z_2 less than the average atomic number of the system, while at small impact parameters and high-charge states, the effective Z_2 is higher than the average which im-

plies interactions with more than one of the molecular constituents.

The physical picture implies, in the case of single-electron loss, that such interactions occur primarily in large-impact-parameter collisions with peripheral atoms of the molecule. Because of geometrical effects, such as shadowing and correlated interaction effects of the individual constituents with the projectile, the effective atomic number Z_2 is generally less than the average of the system. This picture changes for lower impact-parameter collisions which may involve more than one atom of the system and thus to higher effective atomic numbers. Due to the high-collision frequencies of such interactions, multiple-electron losses may be enhanced due to collisional

excitations followed immediately by other collisions before radiative decay takes place. This gives rise to the so-called "density" effect.

As a matter of practical consideration, the molecular data clearly indicate that complex molecular targets are much more efficient in removing electrons than an atomic target with atomic number equivalent to that of the average of the molecular system.

ACKNOWLEDGMENT

This research is supported by the U.S. Department of Energy, Division of Basic Energy Sciences under Contract No. W-7405-eng-26 with Union Carbide Corporation.

*Murray State University, Murray, Kentucky.

†University of Sussex, Sussex, Brighton, England.

‡University of Connecticut, Storrs, Conn.

§Naval Surface Weapons, White Oak, Silver Spring, Maryland.

¹C. D. Moak, IEEE Trans. Nucl. Sci. NS-19, No. 2, 243 (1972).

²C. D. Moak, IEEE Trans. Nucl. Sci. NS-23, No. 2, 1126 (1976).

³V. S. Nikolaev, Usp. Fiz. Nauk. 85, 679 (1965) [Sov. Phys. Usp. 8, 269 (1965)].

⁴H. D. Betz, Rev. Mod. Phys. 44, 465 (1972).

⁵G. D. Alton, J. A. Biggerstaff, L. Bridwell, C. M. Jones, Q. Kessel, P. D. Miller, C. D. Moak, and B. Wehring, IEEE Trans. Nucl. Sci. NS-22, 1685 (1975).

⁶C. D. Moak, L. B. Bridwell, H. A. Scott, G. D. Alton, C. M. Jones, P. D. Miller, R. O. Sayer, Q. C. Kessel, and A. Antar, Nucl. Instrum. Methods 150, 529 (1978).

⁷H. Knudsen, C. D. Moak, C. M. Jones, P. D. Miller, R. O. Sayer, G. D. Alton, and L. B. Bridwell, Phys. Rev. A 19, 1029 (1979).

⁸R. A. Spicuzza and Q. C. Kessel, Phys. Rev. A 14, 630 (1976).

⁹S. Datz, C. D. Moak, H. O. Lutz, L. C. Northcliffe, and L. B. Bridwell, At. Data 2, 273 (1971).

¹⁰V. S. Nikolaev and I. S. Dmitriev, Phys. Lett. 28A, 277 (1968).

¹¹R. O. Sayer, Rev. Phys. Appl. 12, 1543 (1977).

¹²W. E. Lamb, Phys. Rev. 58, 696 (1940).

¹³N. Bohr, Phys. Rev. 58, 654 (1940).

¹⁴N. Bohr, Phys. Rev. 59, 270 (1941).

¹⁵J. H. Brunings and J. K. Knipp, Phys. Rev. 59, 919 (1941).

¹⁶J. H. Brunings, J. K. Knipp, and E. Teller, Phys. Rev. 60, 567 (1941).

¹⁷N. Bohr, K. Dan. Vidensk. Selsk. Mat. Fys. Medd. 18, No. 8 (1948).

¹⁸N. Bohr and J. Lindhard, K. Dan. Vidensk. Selsk. Mat. Fys. Medd. 28, No. 7 (1954).

¹⁹H. A. Scott, L. B. Bridwell, C. D. Moak, G. D. Alton, C. M. Jones, P. D. Miller, R. O. Sayer, Q. C. Kessel, and A. Antar, Phys. Rev. A 18, 2459 (1978).

²⁰J. R. Macdonald, S. M. Ferguson, T. Chiao, L. D. Ellsworth, and S. A. Savoy, Phys. Rev. A 5, 1188 (1972).

²¹S. M. Ferguson, J. R. Macdonald, T. Chiao, L. D. Ellsworth, and S. A. Savoy, Phys. Rev. A 8, 2417 (1973).

²²T. Tonuma, I. Kohno, Y. Miyazawa, F. Yoshida, T. Karasawa, T. Takahashi, and S. Konno, J. Phys. Soc. Jpn. 34, 148 (1973).